PII: S0032-3861(97)00589-2

Polymer Vol. 39 No. 14, pp. 3273–3277, 1998

0032-3861/98/$19.00+0.00

Molecular microstructure dependence of space charges in polymers. Study by the thermal step method of hydrogenated poly(vinyl chloride) as a precursor of polyethylene

N. Guarrotxena[a], N. Vella[b], A. Toureille[b] and J. L. Millán[a,*]

[a]*Instituto de Ciencia y Tecnología de Polímeros (ICTP-CSIC), Juan de la Cierva 3, Madrid 28006, Spain*

[b]*Laboratoire d'Electrotechnique (UM2), Case Courier 079, Place Eugène Bataillon 34095, Montpellier Cedex 5, France*

(Received 19 March 1997; accepted 14 July 1997)

The space charge distribution, an important electrical property, has been studied by means of the thermal step (TS) method for some poly(vinyl chloride) (PVC) samples containing polyethylene (PE) sequences, as the result of hydrogenation reaction of PVC with H_4LiAl to conversions ranging from 1 to 12%. Both the preparation and the characterization of the samples by ^{13}C n.m.r. are to be published elsewhere. The aim of the present work is to investigate the effect of the changes in molecular microstructure, whether relevant to the tacticity of PVC or to that occurring when CH_2 groups are substituted for CHCl groups, on the nature and distribution of space charges which are formed upon applying an electrical field. The contribution of the PE structure to the overall space charge distribution could be evidenced by comparing the results obtained to those extensively published on tacticity-microstructure/space charge relationships for PVC. Since hydrogenated PVC may be considered as a precursor of PE, the results provide novel information about the space charge behaviour of the latter polymer.

(Keywords: hydrogenated PVC-space charges; tacticity-microstructure; composition-microstructure)

INTRODUCTION

A considerable amount of research work in our laboratory (ICTP) has been directed at proving the relationship between the so-designated 'tacticity-microstructure' of poly(vinyl chloride) (PVC). On the one hand, a series of chemical behaviours have been investigated, e.g. the mechanisms of thermal degradation[1] and analogous chemical reactions[2,3] and, on the other, some physical properties[4–6]. Of the latter, the space charges trapped after applying an electrical field have been the major concern of recent publications[7–9].

The specific details of the 'tacticity-microstructure' concept have been widely conveyed[2,3]. It refers to a number of structural local peculiarities along the polymer chain induced by the tacticity without the occurrence of any change in the chemical composition. The most salient are the isotactic tetrad *mmr* (meso–meso–racemic) and the heterotactic pentad *rrmr* (racemic–racemic–meso–racemic) which lie necessarily by the side of isotactic and syndiotactic sequences respectively, regardless of their length[2,3]. In addition, the probable chain conformations of *mmr*, namely GTTG'TT and GTGTTT, are of great importance.

The progressive removal of the above structures, whether through stereospecific nucleophilic substitution[2,3] or by stretching of films so as to provoke some definite conformational changes[9], enabled the availability of model-polymers with well-known tacticity-microstructure, thereby making it possible to study the microstructure/property correlations.

As regards the space charges produced in the polymer upon application of an electrical field, a property of great importance for the insulating materials[10], some original correlations have been recently obtained by comparing the amount and distribution of such charges as measured by the thermal step method[11–13] of the two above-mentioned series of model-samples of PVC[8,9]. Basically, it has been shown that those quantities relate both to the content of the *mmr* structures and to the conformation that they are taking. However, the charges were found to stem from polarization (heterocharges) rather than from injection (homocharges) even if some injection was detected on the anode[8].

Since the hydrogenation reaction of PVC is also stereoselective in the way that it occurs preferably by the *mmr* structure terminal of isotactic sequences, at least up to about 10% conversion[2,3], it appeared to be of great interest to perform a similar study with a PVC after reduction to degrees between 0 and 12.3 mol%. Indeed, reduction of PVC involves the removal of *mmr* structures by exchanging them for ethylene units. Thus, the space charge behaviour of hydrogenated PVC is expected not only to give further support for the effect of the tacticity-microstructure, but also to give information as to the nature and distribution of space charges in polyethylene (PE), a non-polar material, compared to PVC even if some PVC parts in hydrogenated

* To whom correspondence should be addressed

PVC will increase the space charge density. An attempt to provide some reliable answers to this problem is described.

EXPERIMENTAL

Materials

Sample A was an additive-free commercial PVC prepared in bulk polymerization at 70°C; the process was stopped at conversion 62%. The number-average molecular weight ($M_n = 44 \times 10^3$) was determined osmometrically at 34°C with solutions in cyclohexanone using a Knauer membrane osmometer.

Cyclohexanone was purified by fractional distillation under nitrogen. Tetrahydrofuran (THF) was distilled under nitrogen with lithium aluminium hydride (Merck) immediately before use to remove peroxide.

Hydrogenation reaction with H_4LiAl

The hydrogenation reactions of PVC (sample A) with H_4LiAl in THF solution were carried out at 40°C in an atmosphere of purified nitrogen. The samples B–F were purified twice by precipitation from THF in methanol, washed and finally dried under vacuum at 50°C.

The degree of hydrogenation was determined by ^{13}C n.m.r. spectroscopy.

^{13}C n.m.r. spectroscopy

The tacticity of samples A–F was measured by means of ^{13}C n.m.r. decoupled spectra obtained at 85°C on an XL-300 Varian instrument, operating at 75.5 MHz using 1,4-dioxane-d_8 as solvent. The spectral width was 2500 MHz, and a pulse repetition rate of 3 s and 16K data points were used. The relative peak intensities were measured from the integrated peak area, calculated by means of an electronic integrator. The results are given in *Table 1*.

Preparation of the films

Films of thickness 160 μm (samples A–D), 120 μm (sample E) and 220 μm (sample F) were made by compression moulding at 150°C at a pressure of 125 bar, using a Collin press Model 300.

Thermal step (TS) method

The specific details of this method have been published[11–13].

Let us consider *Figure 1*, an insulating material with a constant thickness D and two electrodes on its external faces with an effective area S (it can be a slab or a cylinder).

From the total influence principle ($D \ll \sqrt{S}$), a space charge Q_i, located at x from one electrode, and at $D - x$ from the other one induces image charges Q_1 and Q_2 in the electrodes. This principle is expressed by:

$$Q_i + Q_1 + Q_2 = 0$$

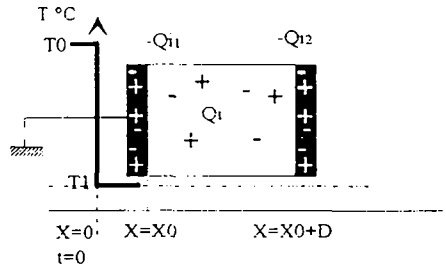

Figure 1 The principle of the thermal step method

The experiment is done in short-circuit so we obtain:

$$\int_{x_0}^{x_0+D} E(x)\,dx = 0$$

The sample is at room temperature. The temperature of one side of the sample is then suddenly cooled to −10°C while the other side is kept at room temperature. The diffusion of this thermal step ($\Delta T = -35$°C) through the insulator creates a variation of $Q_i(x)$ which is made by the expansion of the material and induces a variation of image charges Q_2 (and Q_1). This gives rise to a current expressed as follows:

$$I(t) = -dQ_2/dt = -\alpha C_0 \int_{x_0}^{x_0+D} E(x)\,(dT(x,T)/dt)\,dx$$

$$\alpha = \alpha_d - \alpha_\varepsilon;\ \alpha_d = (1/\mu)\,\partial\mu/\partial T;\ \alpha_\varepsilon = (1/\varepsilon)\,\partial\varepsilon/\partial T$$

where C_0 is the capacity of the sample, α_d is the expansion coefficient of the sample, α_ε is the temperature coefficient of the permittivity ε and x_0 is the equivalent thickness between the thermal source and the sample face.

The space charge distributions are calculated from the current by a deconvolution algorithm developed by Toureille and co-workers[11–13]. The theory and the numeric treatment (Fourier series or derivation) have been described in detail in previous papers[13].

Aluminium electrodes ($\phi = 20$ mm) have been deposited under vacuum on each side of the samples. These were polarized at 50°C for 2 h under an electric field of 10 kV mm^{-1}.

Space charge measurements were performed after a short-circuit of 44 h. This period was usual in earlier work regardless of the type of polymer after proving that no change in space charge density occurs.

Table 1 Characteristics of polymers[a]

Sample	Hydrogenation degree (mol%)	Tacticity		
		mm (%)	*mr* (%)	*rr* (%)
A	0	20	49.7	30.3
B	1.3	18.5	49.3	32.2
C	3.4	18.1	48.5	33.4
D	7.1	16.6	48.5	34.9
E	9.4	15.6	49.2	35.2
F	12.3	14.8	49.2	36

[a]Values taken from [14]
mm: isotactic triad
mr: heterotactic triad
rr: syndiotactic triad

RESULTS AND DISCUSSION

The plots of current intensity *versus* time as obtained from the TS method in the anode and the cathode are displayed in *Figure 2*. All the values of the thickness of the film have been normalized to a constant value of 160 μm. This is the real thickness of most of the films. The curves exhibit a similar shape irrespective of the hydrogenation degree.

From mere inspection it follows that the overall current intensity varies with hydrogenation but not in a progressive way. This is better observed in *Figure 3* showing the maxima of *Figure 2* as a function of hydrogenation degree. Clearly there are three types of behaviour. First, the intensity current of PVC increases in either electrode up to as low a hydrogenation as 1.3%. Then a steady-state of

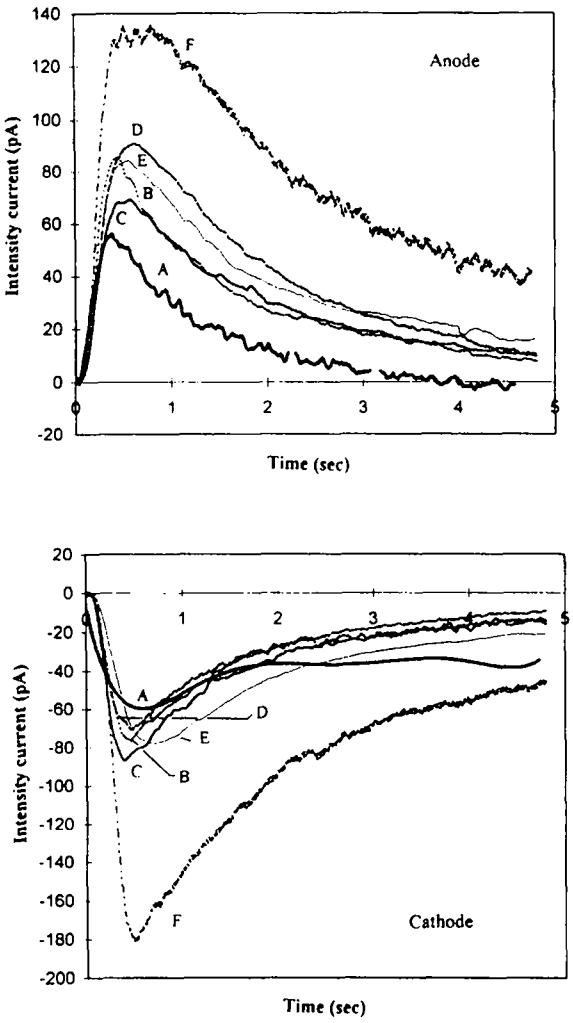

Figure 2 Intensity of the thermal step induced currents *versus* time for PVC hydrogenated to various degrees (*Table 1*): (A) 0%; (B) 1.3%; (C) 3.4%; (D) 7.1%; (E) 9.4%; (F) 12.3% (10 kV mm $^{-1}$, 50°C, 2 h)

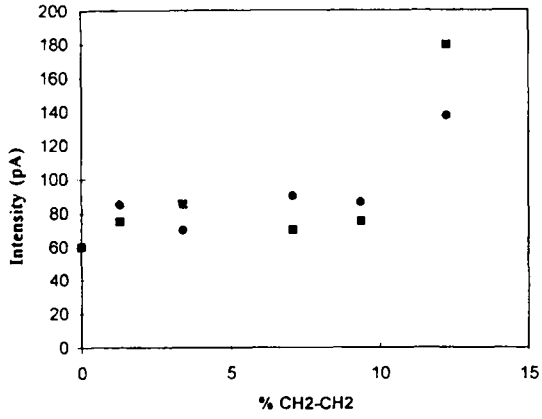

Figure 3 Evolution of the current intensity at the maxima of *Figure 2* with degree of hydrogenation: ●, anode; ■, cathode

the null slope of about 9.4% holds up to conversion, after which the trend with increasing hydrogenation is towards a strong increase, particularly in the cathode.

The behaviour of *Figure 3* is at variance with that obtained for the same PVC sample after the nucleophilic substitution reaction in cyclohexanone solution to conversions within the same range as the hydrogenation one (*Table 1*). Indeed, the intensity decreased strongly up to 1.1% conversion, then from 1.1 to 7% it decreased more slowly to attain a steady period of very low slope[8]. According to earlier work this behaviour could be attributed to the disappearance of *mmr* structures at the end of long isotactic sequences under GTTG⁻TT conformation (1.1%) or GTGTTT conformation (7%) and to the disappearance, simultaneously, of the remaining *mmr* structures and of *rrmr* structures at the end of syndiotactic sequences (steady-state) as the result of nucleophilic substitution[8]. The explanation was argued to lie in the distinct excess free volume, local mobility and the inter-chain interaction characteristic of each of the above structures prior to and after nucleophilic substitution[8]. As will be seen later, hydrogenation behaves in a different way to nucleophilic substitution in that the changes in microstructure involved of the hydrogenation of the same PVC structures are significantly different.

In this connection, the steady-state of *Figure 3*, despite the gradual change in microstructure along this period, is to be interpreted as the result of the occurrence of two processes of reverse effect on the overall space charges formed upon application of an electrical field. According to the mechanism of the hydrogenation reaction[14], one process is the removal of *mmr* structures which, as in nucleophilic substitution, would bring about a decrease in intensity of the current curves[8]. Another process is the progressive substitution of CH_2 groups for CHCl groups, that is the substitution of hydrogen atoms for chlorine atoms. Comparing the latter substitution and that of nucleophilic substitution, where the incorporated chemical group is bulkier and of similar polarity to the chlorine atom[8], it is evident that the second process, unlike the first, occurs in different ways for the two substitutions. This could balance the decrease in current intensity resulting from the first process, so justifying the occurrence of the steady period (*Figure 3*). Note that these processes relate to the tacticity-dependent microstructure[2,3] and the chemical composition-based microstructure, respectively. The changes in the former structure will occur similarly in both nucleophilic substitution and hydrogenation, contrary to what happens in the latter structure.

In light of these competing processes, the three distinct periods shown in *Figure 3* may be assumed to agree with the changes in the overall molecular microstructure found in the hydrogenation reaction[14]. In addition, it explains the divergences found compared to nucleophilic substitution[2,3]. Indeed, the *mmr* structures removed from PVC up to conversions of 1.3%, and then up to a range of 6–9%, are the ones at the end of the isotactic sequences equal to or longer than one heptad, taking preferably the GTTG⁻TT and the GTGTTT conformation respectively[2,3]. It is only in the latter conversion range that the reaction occurs by the remaining *mmr* at the end of shorter isotactic sequences and by the *rrmr* structures related to syndiotactic sequences.

As explained before on the basis of nucleophilic substitution[8], the above microstructural events by themselves would have to cause the current intensity to decrease rapidly for sample B and then to slow down to attain a steady-state of low but negative slope. Clearly this is at variance with what really occurs (*Figure 3*). As already pointed out, the explanation lies in the fact that the evolution of the chemical composition-based microstructure is different for both reactions in that hydrogenation, unlike nucleophilic substitution, involves both a marked increase in the capability of C–C bonds to rotate and to depart from stable all-*trans* conformation (appearance of three consecutive CH_2 groups), as well as a strong decrease in dipole

content (substitution of hydrogen for chlorine atoms). In addition, these effects are more accentuated as the conversion exceeds 7–9% due to the appearance of PE triads, i.e. sequences of at least six CH_2 groups.

These changes in compositional microstructure, therefore, ought to balance the decrease of free volume and local mobility characteristic of the evolution of tacticity microstructure. (Such a compensating effect occurs in nucleophilic substitution reactions only at high conversions where the reaction by *rrmr* structures prevails over *mmr* structures causing the slope of the plot current intensity degree of substitution to slow to a very low value[8].)

Also, the departures from the steady-state in *Figure 3* are to be assigned to the superiority of the compositional-microstructure, relative to the tacticity-microstructure, in trapping space charges once the *mmr* structures adjacent to long isotactic sequences—whether under GTTG$^-$TT conformation or under GTGTTT conformation—have disappeared as the result of hydrogenation. This is consistent with what happens for samples B (1.3%) and E (9.4%), respectively[14]. In this regard, the strong increase in current intensity between samples E (9.4%) and F (12.3%) agrees with the additional effect of the PE triads which are formed from hydrogenation conversions at around 7%[14].

The results shown thus far clearly indicate not only that tacticity-microstructure of PVC is a space charge-determining feature so confirming earlier work[7–9], but also that the PE sequences resulting from hydrogenation, even at low concentration, strongly alter the space charge behaviour of the samples. This makes it possible to get valuable information about the space charge in PE, an important insulating material, by comparing the behaviour of samples in *Table 1*, which are a progressive transition from PVC to PE.

The space charge distributions obtained through a deconvolution of the measured currents of *Figure 2* are given in *Figure 4*. The deconvolution method utilized has been developed by Toureille *et al.*[12] (see Section 2).

By comparing PVC (*Figure 4*) to similar conversions as those shown in *Table 1* ([8]), both prior to and after the nucleophilic substitution reaction[8], it is evident that the space charge distribution of hydrogenated PVC consists of a polarization profile near either electrode and of a strong distortion in the middle of the film. The former profile is characteristic of PVC; the amplitude for either electrode varies with hydrogenation without changing either the shape or the position of maxima of charge density. As for the distortion in the middle of the film, this is apparently irrespective of the hydrogenation degree and it moves towards the anode side as the latter increases. Taking into account the space charge distribution typical of PVC, such a distortion is to be attributed to the appearance of sequences of at least three consecutive CH_2 groups. The space charge distribution characteristic of PE as obtained by other authors[10] gives support to this correlation.

Accordingly, the patterns of *Figure 4* consist of the overlapping of the space charge distributions typical of PVC and PE as shown in *Figure 5*. Also, by comparing the distributions of samples C, D and E corresponding to the steady-state of *Figure 3*, it is apparent that the relative

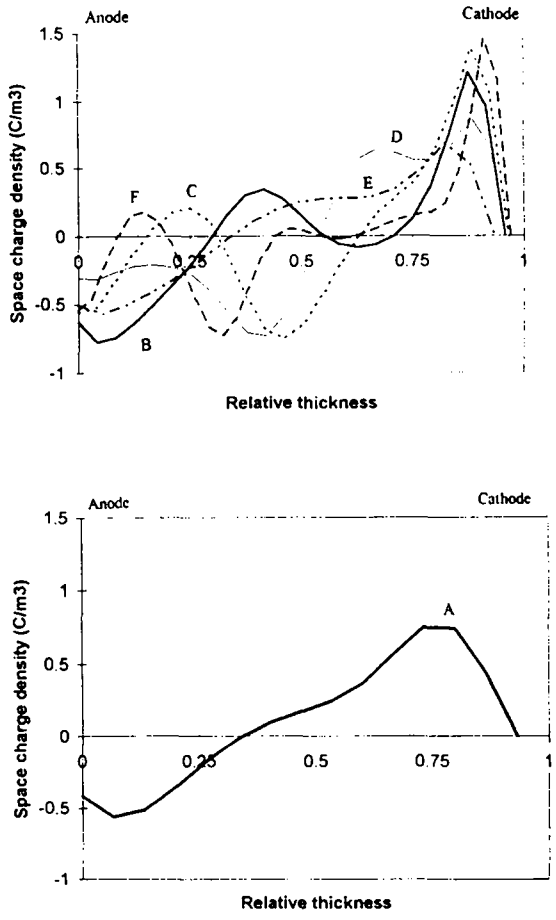

Figure 4 Space charge distribution in polarised PVC hydrogenated to different degrees: *bottom*: (A) 0%; *top*: (B) 1.3%; (C) 3.4%; (D) 7.1%; (E) 9.4%; (F) 12.3% (10 kV mm^{-1}, 50°C, 2 h)

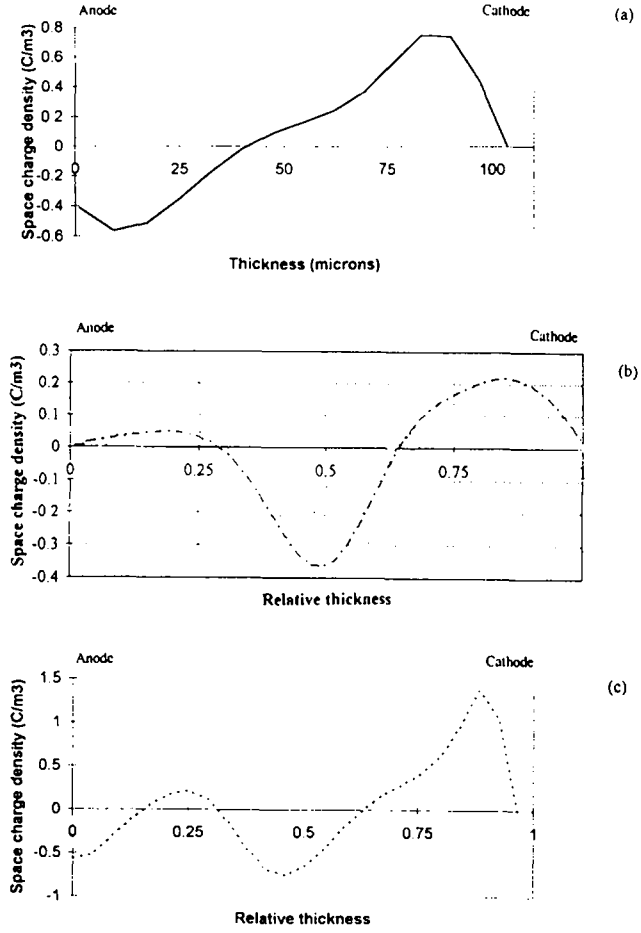

Figure 5 The typical profile of space charge distribution in: (a) PVC; (b) PE (from [10]); (c) hydrogenated PVC

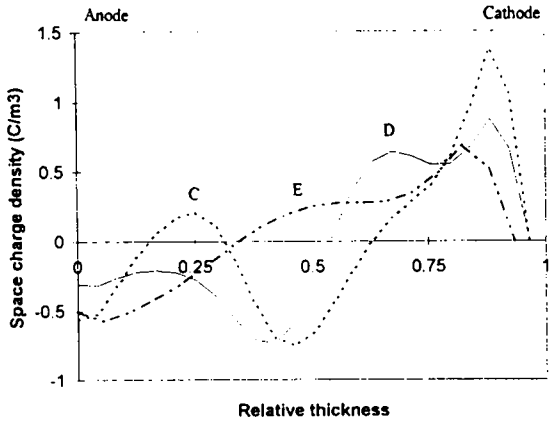

Figure 6 Space charge density in polarized PVC hydrogenated to different degrees: (C) 3.4%; (D) 7.1%; (E) 9.4%; (10 kV mm $^{-1}$, 50°C, 2 h)

contributions of the tacticity-microstructure and of the compositional-microstructure related to PVC and to PE, respectively, are well differentiated (*Figure 6*). This is more indicative as both the electrical field and the temperature utilized when applying the TS method in this work are only on the threshold of those utilized for the profile typical of PE to emerge completely[10]. This is probably the reason why some deviations appear for the samples on the threshold of the steady period of *Figure 3*. Indeed, it has been shown that a low electrical field in PE can hinder, to a substantial extent, the charge injection from the anode, so enhancing the polarization at the cathode[10].

In this respect, *Figure 4* shows that the amplitude near the electrodes varies with hydrogenation; first, it increases up to a certain conversion lying between 3.4 and 7.1%; then it decreases progressively. Taking into consideration the earlier work on PVC[7-9], this behaviour can only be due to the presence of PE units because only continuous changes in intensity—most often towards lower values—were observed in PVC, either after nucleophilic substitution[8] or after physical treatments[9]. In addition, as reflected by the space charge distribution in the middle, the marked contribution of PE units, despite their low proportion relative to PVC units, becomes more apparent as the hydrogenation progresses. This shows the transition from a predominant polarization (heterocharges) pattern in either electrode to a profile revealing injection from the anode (homocharges) and polarization near the cathode (heterocharges). The latter is known to be characteristic of PE[15].

More conclusive details of the molecular microstructure–space charge relationships are to be provided by a parallel investigation, which will be published shortly. It includes: the Thermal Stimulated Discharge Currents (TSDC) study of samples of *Table 1*; the influence of the electrical field strength on the space charge profile as obtained by the Thermal Step (TS) method for some of the samples (*Table 1*); and the application of the so-called 'peak-cleaning' technique[16] to determine the presence and quantity of the injection charges which are masked by the majority charges derived from polarization. Such courses of action will allow one to state the contribution of PE units to the whole space charge profile obtained for PVC after hydrogenation.

Be that as it may, the results obtained herein confirm the conclusions of earlier work on the tacticity-microstructure–space charge relationships. In addition, they provide valuable information about the space charge behaviour of PE through the gradual structural transition from PVC to PE as the result of the hydrogenation of the former. This is all the more interesting as the direct studies on PE cannot convey data of the specific molecular dependence of space charge generation upon applying an electrical field. On the other hand, studying the evolution of space charge of PVC after chemical modification proves highly useful to differentiate the role of tacticity-microstructure and of chemical composition microstructure in that electrical property, even though as is the case in samples of *Table 1*, the content of PE units relative to PVC is very low.

CONCLUSIONS

In addition to these general contributions the following specific conclusions are to be highlighted: (1) the plateau in the plot of peak current *versus* percentage of CH_2–CH_2, due to the competing processes of removal of *mmr* structures and the substitution of CH_2 for CHCl, confirms the crucial role of both types of molecular microstructure in the space charge behaviour of polymers; (2) charge density near the electrodes follows hydrogenation as a result of the enhanced polarizability of the remanent PVC parts; and (3) total charge distribution, to some extent, is the summation of PE and PVC results and is very sensitive to the PE content.

REFERENCES

1. Millán, J., Martínez, G., Gómez-Elvira, J. M., Guarrotxena N. and Tiemblo, P., *Polymer*, 1996, **37**, 219, and references cited therein.
2. Guarrotxena, N., Martínez, G. and Millán, J., *J. Polym. Sci.: Polym. Chem.*, 1996, **34**, 2387, and references cited therein.
3. Guarrotxena, N., Martínez, G. and Millán, J., *J. Polym. Sci.: Polym. Chem.*, 1996, **34**, 2567, and references cited therein.
4. Tiemblo, P., Martínez, G., Gómez-Elvira, J. M. and Millán, J., *Polym. Bull.*, 1994, **32**, 353.
5. Guarrotxena, N., Martínez, G., Gómez-Elvira, J. M. and Millán, J., *Macromol. Rapid Commun.*, 1994, **15**, 189.
6. Guarrotxena, N., Martínez, G. and Millán, J., *Polymer*, 1997, **38**(8), 1857.
7. Vella, N., Toureille, A., Guarrotxena, N. and Millán, J., *Macromol. Chem. Phys.*, 1996, **197**, 1301.
8. Guarrotxena, N., Vella, N., Toureille, A. and Millán, J., *Macromol. Chem. Phys.*, 1997, **198**, 457.
9. Guarrotxena, N., Vella, N., Toureille, A. and Millán, J., *Polymer*, 1997, **38**, 4253.
10. Vella, N., Doctorate thesis, Institut National Polytechnique de Tolouse, 1996.
11. Toureille, A., *Jicâble*, 1987, **87**, 89.
12. Cherifi, A., Abbou Dakka, M. and Toureille, A., *IEEE Trans. Electr. Insul.*, 1992, **27**, 1152, and references cited therein.
13. Toureille, A., Reboul, J. P. and Merle, P., *J. Phys. III*, 1991, **1**, 111.
14. Contreras, J., Doctorate thesis, Universidad Complutense de Madrid, 1997.
15. Vella, N., Toureille, A. and Zebouchi, N. H., and the Giam, H., *REE Special Cables et isolants*, 1996, p. 102.
16. Creswell, R. A. and Perlmann, M. M., *J. Appl. Phys.*, 1971, **42**, 2645.